Journal of Applied Electrochemistry **31**: 1055–1060, 2001.

Electrode reaction of the Np^{3+}/Np couple in LiCl–KCl eutectic melts

O. SHIRAI[1]*, M. IIZUKA[2], T. IWAI[1] and Y. ARAI[1]
[1]*Department of Nuclear Energy System, Japan Atomic Energy Research Institute, Oarai-machi, Higashiibaraki-gun, Ibaraki-ken, 311-1394 Japan*
[2]*Nuclear Fuel Cycle Department, Central Research Institute of Electric Power Industry, Tokyo, 201-8511 Japan*
*(*author for correspondence)*

Received 6 February 2001; accepted in revised form 27 May 2001

Key words: chronopotentiometry, cyclic voltammetry, electrode reaction, electromotive force, LiCl–KCl eutectic salt, molybdenum, neptunium

Abstract

The electrochemical behaviour of the Np^{3+}/Np couple in the LiCl–KCl eutectic salt was investigated by electromotive force measurements, cyclic voltammetry and chronopotentiometry in the temperature region between 723 and 823 K. The standard redox potential of the Np^{3+}/Np couple vs Ag/AgCl (1.00 wt %) was measured and given by the equation, $E^{\circ}_{Np^{3+}/Np} = -2.0298 + 0.000706\ T$, where E is in V and T in K. The electrode reaction of the Np^{3+}/Np couple was almost reversible under the conditions studied. The diffusion coefficient of Np^{3+}, $D_{Np^{3+}}$, in the LiCl–KCl eutectic melts between 723 and 823 K was represented by the equation, $D_{Np^{3+}} = 2.22 \times 10^{-6} - 6.88 \times 10^{-9}\ T + 5.60 \times 10^{-12}\ T^2$ cm^2 s^{-1}. The adsorption and desorption peaks of Np at the Mo working electrode caused by underpotential deposition were also observed in the cyclic voltammograms, and the work function of Np was evaluated as 3.04 eV by peak analysis of the cyclic voltammograms.

1. Introduction

Pyrochemical reprocessing of nuclear fuels using molten salt as a solvent shows promise for advanced nuclear engineering because of its compactness, economy, radiation resistance and compatibility with nonproliferation [1]. In the electrorefining process, which is a key step in pyrochemical reprocessing, spent fuels are anodically dissolved in LiCl–KCl eutectic melt, and U, Pu and minor actinides (MAs; Np, Am, Cm etc.) are recovered together at a cathode [2, 3]. There is little electrochemical data on MAs in LiCl–KCl eutectic melt, although MAs need to be recovered from high level wastes in order to develop the transmutation technology of long-lived MAs.

For Np, which is one of the long-lived MAs, the electrode reaction of the Np^{3+}/Np redox couple in LiCl–KCl eutectic melts has been investigated by several authors [4–8]. Martinot et al. [4–6] reported that the standard potentials of the Np^{3+}/Np couple vs Cl_2/Cl^- (reference electrode) were −2.378, −2.342, −2.315 and −2.281 V at 673, 723, 773 and 823 K, respectively, and that the electrode reaction of the Np^{3+}/Np couple was nearly reversible. On the other hand, the redox standard potentials of the Np^{3+}/Np couple vs Cl_2/Cl^- (reference electrode), which were measured by Roy et al. [7], were −2.845, −2.827, −2.808 and −2.775 V at 673, 698, 723 and 773 K, respectively. Krueger et al. [8] reported that these standard redox potentials at 673, 723 and 773 K were −2.725, −2.697 and −2.660 V, respectively. There is therefore a gap among the reported values of the standard redox potential of the Np^{3+}/Np couple.

From the analysis of the chronopotentiogram, Martinot and Duyckaerts [6, 8] reported that the diffusion coefficient of Np^{3+} in LiCl–KCl eutectic melt increased from 4.6×10^{-6} to 26.9×10^{-6} cm^2 s^{-1} with an increase in temperature from 673 to 923 K. Martinot et al. [6, 9, 10] reported that the diffusion coefficients of U^{3+} and Pu^{3+} in LiCl–KCl eutectic melt were nearly equal to those of Np^{3+}. However, the diffusion coefficients of U^{3+} in NaCl–KCl eutectic melt, which obtained by Serrano and Taxil [11], and those of Pu^{3+} in LiCl–KCl eutectic melt, which reported by Leseur [12] and Nissen [13], are several times larger than those by Martinot et al.

In the present work cyclic voltammograms of the Np^{3+}/Np couple in the LiCl–KCl eutectic salt were obtained, and the redox potentials of the Np^{3+}/Np couple and the diffusion coefficients of Np^{3+} in the LiCl–KCl eutectic melt were evaluated by potentiometric methods in the temperature range 723 to 823 K.

2. Experimental details

The electrochemical cell used for the voltammetric studies was described previously [14]. An Mo wire of 1.0 mm in diameter served as a working electrode. The Mo wire was encased in a high-purity alumina tube in such a way that an apparent surface area of 0.322 cm^2 was exposed to the molten salt. A silver–silver chloride (Ag/AgCl) electrode used as a reference electrode consists of a closed-end mullite tube (50% Al_2O_3 + 46% SiO_2; Nikkato Co.) in which LiCl–KCl eutectic salt containing 1.00 wt % AgCl was placed and an Ag wire of 1 mm in diameter was immersed in the salt. A glassy carbon (99.998% GC; Tokai Carbon Co., Ltd) rod of 3.0 mm in diameter and 15 mm length was used as a counter electrode. The temperature of the molten salt was measured to ±0.5 K by a calibrated chromel–alumel thermocouple immersed in the electrolyte. Cyclic voltammograms were measured using a voltammetric analyzer BAS CV-50W. Electromotive force measurements and chronopotentiograms were recorded using a potentiostat/galvanostat HA-501 (Hokuto Denko Co.), a function generator HB-104 (Hokuto Denko Co.) and a X–t recorder 3023 (Yokogawa Electric Co.).

Polarographic-grade LiCl–KCl eutectic was obtained from the Anderson Physics Laboratory. Mo (> 99.95%) was available from Soekawa Chemicals Co. Neptunium trichloride was prepared by the chlorination of $NpPt_3$ with $CdCl_2$ (> 99.99%; Anderson Physics Laboratory) in the LiCl–KCl/Cd system at 773 K, which produced yellow salts containing about 20 wt % $NpCl_3$ [15]. $NpPt_3$ was synthesized by heating the mixture of NpN, which was prepared by carbothermic reduction of NpO_2 [16], and Pt powders (> 99.95%; Rare Metallic Co.) in Ar gas (> 99.999%) stream at 1073 K for 21.6 ks. In the carbothermic reduction, the mixture of NpO_2 and graphite powder with a C/NpO_2 molar ratio of 2.5 was heated at first in N_2 gas stream at 1823 K and then in 92% N_2–8% H_2 mixed gas stream at 1823 K. Salt containing about 20 wt % $NpCl_3$ obtained in the above-mentioned procedure was diluted by the addition of the LiCl–KCl eutectic melt in order to obtain the adequate concentration of $NpCl_3$ for the electrochemical measurement. The concentration of $NpCl_3$ in the LiCl–KCl eutectic melts was determined by ICP–AES.

The voltammetric measurements were carried out in a glovebox with a high-purity argon gas atmosphere (H_2O, O_2 < 2.0 ppm).

3. Results and discussion

3.1. *Redox reaction of Np^{3+}/Np couple at the solid electrode*

Figure 1 indicates a typical cyclic voltammogram obtained with 0.333 wt % $NpCl_3$ in LiCl–KCl eutectic salt at the Mo electrode at 723 K with a potential scanning rate of 0.01 V s^{-1}. Two cathodic (c1, c2) and two anodic (a1, a2) current waves were observed in the cyclic voltammogram. An approximately linear relationship exists between the cathodic peak current c1 and the square root of the potential scanning rate, v, in the region between 0.01 and 0.05 V s^{-1}, though the cathodic peak increased nonlinearly with v in the region of potential scanning rate above 0.1 V s^{-1}, as shown in Figure 2. This nonlinearity might be caused by adsorption of Np metal and overpotential deposition owing to nucleation and crystallization of deposited Np metal. The peak height of c1 in the voltammograms with 0.333, 0.381, 0.430 and 0.465 wt % $NpCl_3$ was approximately proportional to the concentration of $NpCl_3$, as shown in Figure 3. The peak height of c1 was approximately proportional to the concentration of $NpCl_3$. The num-

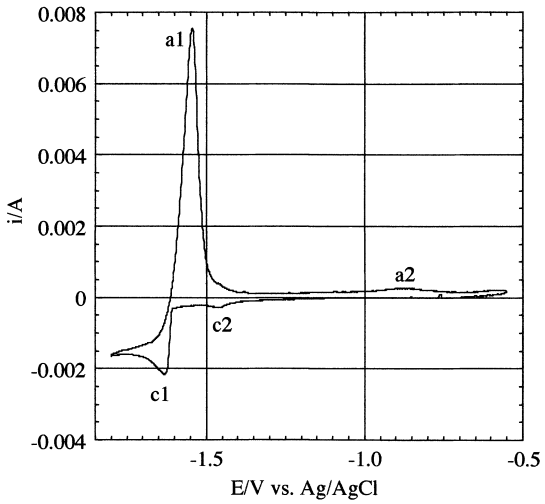

Fig. 1. Cyclic voltammogram for redox reaction of the Np^{3+}/Np couple at the Mo electrode at 773 K. Potential scanning rate = 0.01 V s^{-1}; $NpCl_3$ concentration 0.333 wt %; apparent area of Mo electrode 0.322 cm^2.

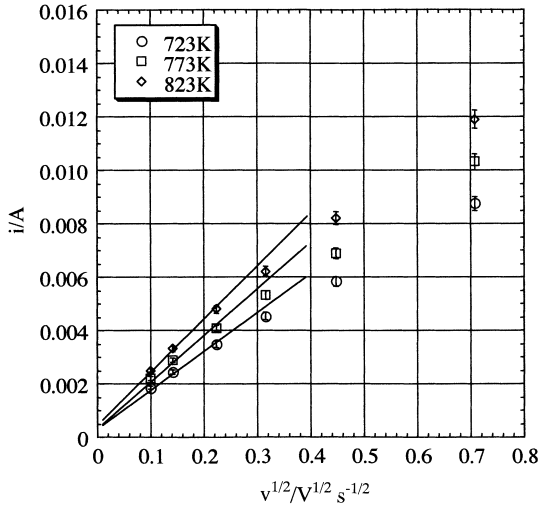

Fig. 2. Plot of cathodic peak current against square root of potential scanning rate (v) on cyclic voltammograms for redox reaction of the Np^{3+}/Np couple at the Mo electrode at 723, 773 and 823 K. $NpCl_3$ concentration 0.333 wt %; apparent area of Mo electrode 0.322 cm^2.

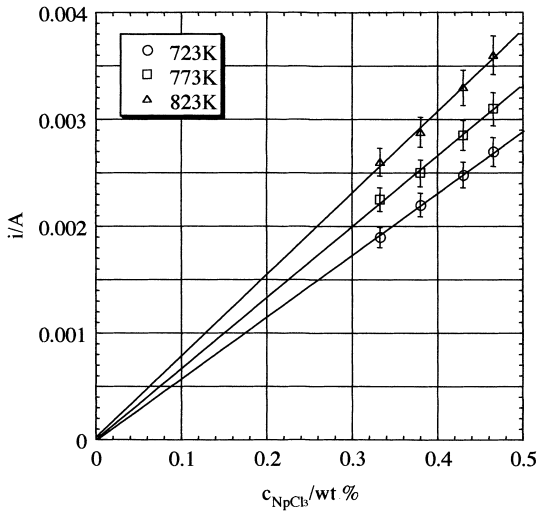

Fig. 3. Plot of cathodic peak current against $NpCl_3$ concentration (c_{NpCl_3}) on cyclic voltammograms for the redox reaction of the Np^{3+}/Np couple at the Mo electrode at 723, 773 and 823 K. Potential scanning rate 0.01 V s^{-1}; apparent area of Mo electrode 0.322 cm^2.

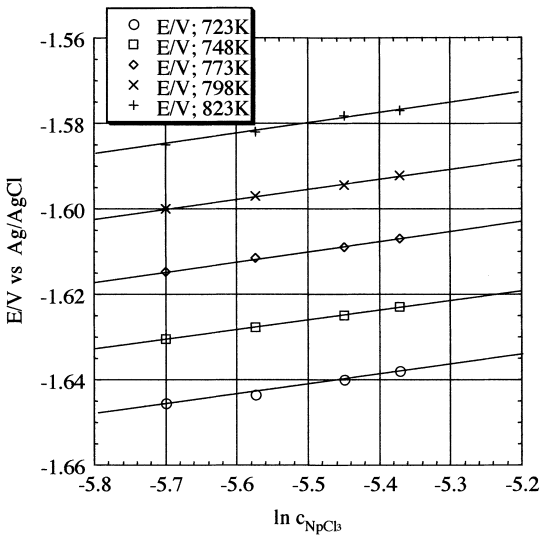

Fig. 4. Equilibrium potentials of the redox reaction of the Np^{3+}/Np couple as a function of natural logarithms of $NpCl_3$ concentration (ln c_{NpCl_3}). Lines drawn by least-squares method with theoretical slope of $RT/3F$.

ber of the transferred electrons, n, was evaluated to be 3.0 ± 0.1 from the slope analysis of the relation between the concentration of $NpCl_3$ and the equilibrium potentials obtained by the measurement of electromotive force as shown in Figure 4 [17]. By considering the above characteristics, the cathodic and the anodic peaks (c1 and a1) correspond to a redox couple given by Equation 1.

$$Np^{3+} + 3e^- = Np \quad (1)$$

The peak heights of c1 at 823 K were about 1.35 times larger than those at 723 K. This temperature dependence might be compatible with the fact that the redox reaction is controlled by diffusion, because the diffusion coefficient of Np^{3+} in LiCl–KCl eutectic at 823 K is about 1.9 times larger than that at 723 K, as presented subsequently.

The potential differences, $\Delta E_{c1-a1,P}$, between the potential of the cathodic peak c1, $E_{c1,P}$, and that of the anodic peak a1, $E_{a1,P}$, were about twice as large as those evaluated theoretically from following relation; $\Delta E_{c1-a1,P} = 2.2\ RT/nF$, where R is gas constant, T temperature, and F Faraday's constant [17]. However, the potential differences, $\Delta E_{c1,P-P/2}$, between the half peak potential of peak c1, $E_{c1,P/2}$, and $E_{c1,P}$ were 0.010–0.015 V smaller than those evaluated theoretically. $E_{c1,P}$ was shifted slightly in the negative direction with an increase in potential scanning rate, but $E_{a1,P}$ was almost constant. These characteristics indicate that the influence of overpotential owing to nucleation and crystallization of deposited Np metal cannot be neglected [18], though the anodic reaction is rapid. Accordingly, potentiometric methods such as the measurement of electromotive force and chronopotentiometry were applied in order to take accurate values of the redox potential of the Np^{3+}/Np couple as below.

The redox potentials of the Np^{3+}/Np couple, $E_{Np^{3+}/Np}$, in the LiCl–KCl melt containing 0.333, 0.381, 0.430 and 0.465 wt % $NpCl_3$ at 723, 748, 773, 798 and 823 K, which were obtained by the measurement of electromotive force, are shown in Figure 4. In the Figure, the standard potentials, $E^\circ_{Np^{3+}/Np}$, for 723, 748, 773, 798 and 823 K, as presented in Table 1, could be obtained by extrapolation of the linear E vs ln c_{PuCl_3} plot to the intercept. Since a plot of $E^\circ_{Np^{3+}/Np}$ against T is found to be linear, as shown in Figure 5, the standard potential vs. the Ag/AgCl electrode may be expressed in the temperature range between 723 and 823 K by Equation (2).

Table 1. Standard potentials, E°, for the Np^{3+}/Np redox couple in LiCl–KCl eutectic salt

Temp. /K	E°/V		ΔG°_f/kJ mol^{-1} electrochem.	E°/V		
	vs Ag/AgCl	vs Cl_2/Cl^-		Martinot et al.	Roy et al.	Krueger et al.
673				−2.378	−2.725	−2.725
698					−2.714	−2.715
723	−1.5191	−2.7155	−786.03	−2.342	−2.698	−2.697
748	−1.5017	−2.7027	−782.30			
773	−1.4845	−2.6900	−778.63	−2.315	−2.668	−2.660
798	−1.4672	−2.6771	−774.91			
823	−1.4474	−2.6619	−770.50	−2.281		

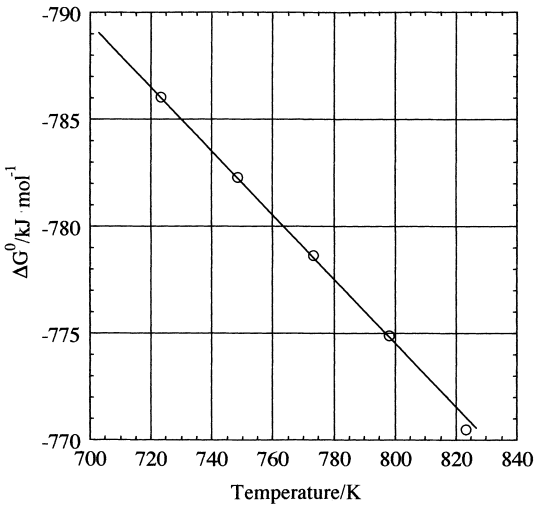

Fig. 5. Standard free energies of formation of $NpCl_3$ in the salt as a function of temperature.

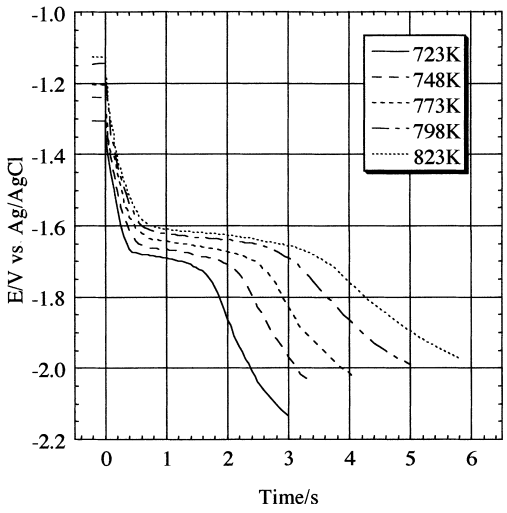

Fig. 6. Chronopotentiograms for the redox reaction of the Np^{3+}/Np couple at the Mo electrode at 723, 748, 773, 798 and 823 K. Applied currents 0.005 A; $NpCl_3$ concentration in the salt 0.333 wt %; apparent area of the Mo electrode 0.322 cm^2.

$$E^{\circ}_{Np^{3+}/Np} = -2.0298 + 0.000706\,T(\text{V vs Ag/AgCl}) \tag{2}$$

where T is in K. The standard redox potential of the Np^{3+}/Np couple in the present result agrees with the literature values reported by Roy et al. [7] and Krueger et al. [8], but the present data differ from Martinot's results [4–6].

By using the data of Yang and Hudson [19] at low AgCl concentrations in the LiCl–KCl eutectic melt, $E^{\circ}_{Np^{3+}/Np}$ can be converted into the standard potential of the Np^{3+}/Np couple vs Cl_2/Cl^- electrode, $E^{\circ}_{Np^{3+}/Np}$ (Cl_2/Cl^-), as shown in Table 1. The standard free energy of formation of $NpCl_3$ in the LiCl–KCl eutectic melt, $\Delta_f G^{\circ}_{NpCl_3}$ (LiCl–KCl), is obtained from the expression;

$$\Delta_f G^{\circ}_{NpCl_3}(\text{LiCl–KCl}) = nFE^{\circ}_{Np^{3+}/Np}(Cl_2/Cl^-) \tag{3}$$

Therefore, $\Delta_f G^{\circ}_{NpCl_3}$ (LiCl–KCl) is expressed by the following equation (with T in K);

$$\Delta_f G^{\circ}_{NpCl_3}(\text{LiCl–KCl}) = -646.1 + 0.027\,T\ (\text{kJ mol}^{-1}) \tag{4}$$

The standard free energy of formation of the solid $NpCl_3$, $\Delta_f G^{\circ}_{NpCl_3}$, has been reported [20], and $\Delta_f G^{\circ}_{NpCl_3}$ values (in kJ mol^{-1}) values in the temperature region from 298.15 to 1000 K can be represented by the following equation:

$$\Delta_f G^{\circ}_{NpCl_3} = -907.586 - 1.20\times10^{-1}\,T - 9.16\times10^{-5}\,T^2 \tag{5}$$

The difference between $\Delta_f G^{\circ}_{NpCl_3}$ and $\Delta_f G^{\circ}_{NpCl_3}$ (LiCl–KCl) can be attributed to both the lattice formation energy of solid $NpCl_3$ and the solvation energy of $NpCl_3$ in the LiCl–KCl eutectic melt, which contains the formation energy of complex ions such as $[NpCl_6]^{3-}$ [7, 12].

3.2. *Diffusion of Np^{3+} in LiCl–KCl eutectic melt*

The chronopotentiograms were obtained by applying 0.005 A between the Mo working electrode and the GC counter electrode in the cell system containing 0.333, 0.381, 0.430 and 0.465 wt % $NpCl_3$, respectively. Figure 6 shows typical chronopotentiograms which were observed at 0.333 wt % $NpCl_3$ in the temperature region between 723 and 823 K. Transition times, τ in s, are noted in Table 2. There exists the relationship expressed by Sand's formula [17];

$$\tau^{1/2} = 0.5\,nF\pi^{1/2}C_0 i_0^{-1} D^{1/2}_{Np^{3+}} \tag{6}$$

where C_0 is bulk concentration of the Np^{3+} (mol cm^{-3}), i_0 is the current density (A cm^{-2}) and $D_{Np^{3+}}$ the diffusion coefficient of the Np^{3+} in LiCl–KCl melt (cm^2 s^{-1}). In the present case, C_0 values may be evaluated from the concentrations of $NpCl_3$ and the densities of the LiCl–KCl eutectic melt [22], therefore 0.333, 0.381, 0.430 and 0.465 wt % could be rewritten as $5.31\times10^{-5} - 5.13\times10^{-8}\,T$, $6.07\times10^{-5} - 5.86\times10^{-8}\,T$, $6.86\times10^{-5} - 6.62\times10^{-8}\,T$ and $7.42\times10^{-5} - 7.17\times10^{-8}\,T$, respectively. Consequently, $D_{Np^{3+}}$ values at 723, 748, 773, 798 and 823 K are $(1.73\pm0.09)\times10^{-5}$, $(2.07\pm0.10)\times10^{-5}$, $(2.48\pm0.15)\times10^{-5}$, $(2.96\pm0.19)\times10^{-5}$ and $(3.48\pm0.23)\times10^{-5}$ cm^2 s^{-1}, respectively, as shown in Table 2. On the other hand, $D_{Np^{3+}}$ values at 723, 773 and 823 K obtained by substituting the current density of the cathodic peak, i_{p0}, in the cyclic voltammograms at 0.010 V s^{-1} into Equation 7:

$$i_{p0} = -0.446\,n^{3/2}F^{3/2}R^{-1/2}T^{-1/2}C_0 D^{1/2}_{Np^{3+}}v^{1/2} \tag{7}$$

Table 2. Transient times (τ) and diffusion coefficients of Np^{3+} in the LiCl–KCl eutectic melt ($D_{Np^{3+}}$)
$i = 0.005$ A, electrode area 0.322 cm^2.

C_{NpCl_3} /wt %	Temp. /K	τ /s	$D_{Np^{3+}}/10^5$ cm^2 s^{-1}	
			Chronopotentiometry	Cyclic voltammetry
0.333	723	1.20 ± 0.05	1.71 ± 0.07	1.69 ± 0.08
	748	1.44 ± 0.05	2.09 ± 0.07	
	773	1.70 ± 0.07	2.50 ± 0.10	2.61 ± 0.13
	798	1.98 ± 0.09	2.96 ± 0.13	
	823	2.31 ± 0.12	3.51 ± 0.18	3.84 ± 0.20
0.381	723	1.60 ± 0.06	1.75 ± 0.07	1.73 ± 0.09
	748	1.90 ± 0.08	2.11 ± 0.09	
	773	2.25 ± 0.10	2.54 ± 0.11	2.51 ± 0.13
	798	2.61 ± 0.13	2.99 ± 0.15	
	823	2.95 ± 0.15	3.44 ± 0.18	3.61 ± 0.18
0.430	723	2.05 ± 0.09	1.75 ± 0.08	1.72 ± 0.09
	748	2.40 ± 0.11	2.08 ± 0.10	
	773	2.80 ± 0.15	2.47 ± 0.13	2.51 ± 0.13
	798	3.26 ± 0.20	2.92 ± 0.18	
	823	3.81 ± 0.23	3.47 ± 0.21	3.44 ± 0.17
0.465	723	2.35 ± 0.10	1.71 ± 0.07	1.74 ± 0.09
	748	2.70 ± 0.13	2.00 ± 0.10	
	773	3.21 ± 0.20	2.42 ± 0.15	2.54 ± 0.13
	798	3.85 ± 0.25	2.95 ± 0.19	
	823	4.50 ± 0.30	3.50 ± 0.23	3.76 ± 0.19

where v is potential scanning rate in V s^{-1}. These values at 723, 773 and 823 K were evaluated as $(1.72 \pm 0.03) \times 10^{-5}$, $(2.53 \pm 0.08) \times 10^{-5}$ and $(3.66 \pm 0.20) \times 10^{-5}$ cm^2 s^{-1}, respectively, and agree very closely with those obtained from the chronopotentiometry. These results are about 2.5 times larger than the $D_{Np^{3+}}$ values obtained by Martinot [4–6]. However, $D_{Np^{3+}}$ values in the present work are in good agreement with the diffusion coefficients of U^{3+} and Pu^{3+}, which were obtained by Serrano and Taxil [11], Leseur [12] and Nissen [13], respectively. Accordingly, it is thought that the present values are of a reasonable magnitude.

When $D_{Np^{3+}}$ values (in cm^2 s^{-1}) at 723, 748, 773, 798 and 823 K are plotted as a function of temperature, a curved line is obtained, as shown in Figure 7. The following equation was obtained from an analysis of the curved line:

$$D_{Np^{3+}} = 2.22 \times 10^{-6} - 6.88 \times 10^{-9}\, T + 5.60 \times 10^{-12}\, T^2 \quad (8)$$

3.3. *Underpotential deposition of Np metal at solid electrode*

The cathodic and anodic peak currents, c2 and a2, increased as the potential scanning rate increased. These peaks were not dependent on the concentration of $NpCl_3$. Though the accumulated amount of charge of c2 or a2 is about 10 times larger than the estimated value of monolayer adsorption or desorption of Np at the surface of Mo electrode, the cathodic c2 and the anodic a2 peaks might be caused by adsorption and desorption

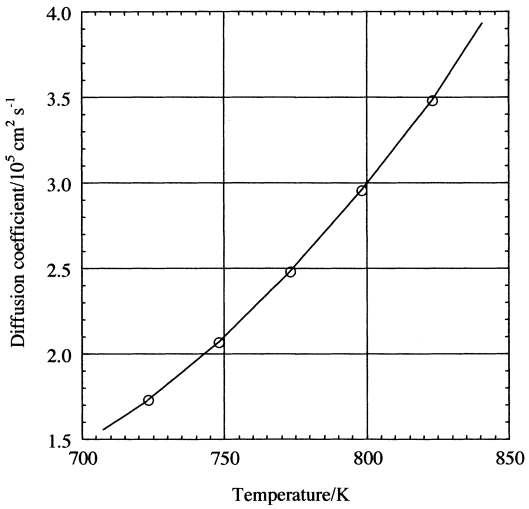

Fig. 7. Diffusion coefficients of Np^{3+} ($D_{Np^{3+}}$) in the salt phase as a function of temperature.

of Np metal on Mo electrode taking into account the above voltammetric behaviors. The behaviour is generally called underpotential deposition. The potentials of the cathodic peak c2, $E_{c2,P}$, in Figure 1 were -1.490 ± 0.020, -1.430 ± 0.020 and -1.370 ± 0.020 V, respectively, and those of a2, $E_{a2,P}$, -0.890 ± 0.010, -0.860 ± 0.010 and -0.830 ± 0.010 V. Since the c2 peaks were broad and $E_{c2,P}$ was shifted to the negative direction with the increase of potential scanning rate, the c2 peaks might be influenced considerably by reaction and crystallization overpotentials [18]. Therefore, the formation energy of a Np–Mo metallic compound at the surface of the Mo electrode can be described by use of the potential differences between $E_{a2,P}$ and $E_{Np^{3+}/Np}$ which were obtained at the same conditions. The potential differences between $E_{a2,P}$ and $E_{Np^{3+}/Np}$ at 723, 773 and 823 K were 0.756 ± 0.010, 0.755 ± 0.010 and 0.755 ± 0.010 V, respectively, and they were almost independent of temperature under the present experimental condition. The underpotential deposition of Np at the surface of the Mo electrode can be correlated to the work functions of electrode material (Mo), ϕ_{Mo}, and deposition metal (Np), ϕ_{Np} [23].

$$\Delta E_{upd} = 0.5 \times (\phi_{Mo} - \phi_{Np}) \quad (9)$$

where ΔE_{upd} is potential difference between $E_{a2,P}$ and $E_{Np^{3+}/Np}$ in V. Since ϕ_{Mo} is 4.55 eV [24], ϕ_{Np} is evaluated at 3.04 V. This value agrees with ϕ_{Np} estimated (3.3 eV) by substituting the electron negativity of Np (1.1) into Equation 10 [25]:

$$x_M = 0.5\,\phi_{Np} - 0.55 \quad (10)$$

where x_M is Pauling's electronegativity [26]. The potential region where the absorption and the desorption peaks appear can be predicted by considering work functions of substrate and deposited materials. When

the molten salt contains plural elements, the effect of codeposition on separation may be predictable.

4. Conclusion

It is found from voltammetric analysis that the electrode reaction of the Np^{3+}/Np couple is almost reversible under the present experimental conditions. The standard redox potential of the Np^{3+}/Np couple obtained by the measurement of electromotive force agrees with the literature values reported by Roy et al. [8] and Krueger et al. [9]. However, the diffusion coefficients of Np^{3+} at 723, 773 and 823 K are about 2.5 times larger than those obtained by Martinot [6, 9, 10], but the diffusion coefficients of Np^{3+} are in good agreement with literature values of U^{3+} and Pu^{3+} which are reported by Serrano and Taxil [11], Leseur [12] and Nissen [13], respectively. The work function of Np can be evaluated as 3.04 eV by peak analysis of cyclic voltammogram.

Acknowledgements

The authors wish to thank Mr K. Shiozawa of JAERI for ICP-AES analysis. We are grateful to Dr K. Franklin of British Nuclear Fuels plc, Dr T. Inoue and Mr Y. Sakamura of CRIEPI, Drs Y. Suzuki, M. Ochiai and Z. Yoshida of JAERI for their interest and useful suggestions.

References

1. Y.I. Chang, *Nucl. Technol.* **88** (1989) 129.
2. J.P. Ackerman, *Ind. Eng. Chem. Res.* **30** (1991) 141.
3. M. Iizuka, T. Koyama, N. Kondo, R. Fujita and H. Tanaka, *J. Nucl. Mater.* **247** (1997) 183.
4. L. Martinot and F. Caligara, *At. Energy Rev.* **11** (1973) 3.
5. L. Martinot, *J. Radional. Nucl. Chem., Lett.* **106** (1986) 135.
6. L. Martinot and G. Duyckaerts, *Anal. Lett.* **1** (1968) 669.
7. J.J. Roy, L.F. Grantham, D.L. Grimmett, S.P. Fusselman, C.L. Krueger, T.S. Storvick, T. Inoue, Y. Sakamura and N. Takahashi, *J. Electrochem. Soc.* **143** (1996) 2487.
8. C.L. Krueger, T.S. Storvick, J.J. Roy, L.F. Grantham, L.R. McCoy, T. Inoue, H. Miyashiro and N. Takahashi, *J. Electrochem. Soc.* **138** (1991) 1186.
9. F. Caligara, L. Martinot and G. Duyckaerts, *Bull. Soc. Chim. Belg.* **76** (1967) 15.
10. L. Martinot and G. Duyckaerts, *Anal. Lett.* **4** (1971) 1.
11. K. Serrano and P. Taxil, *J. Appl. Electrochem.* **29** (1999) 497.
12. R. Leseur, *CEA report, R-3793* (1970).
13. D. Nissen, *J. Inorg. Nucl. Chem.* **28** (1966) 1740.
14. O. Shirai, M. Iizuka, T. Iwai, Y. Suzuki and Y. Arai, *J. Electroanal. Chem.* **490** (2000) 31.
15. O. Shirai, M. Iizuka, T. Iwai, Y. Suzuki and Y. Arai. *J. Nucl. Sci. Technol.* **37** (2000) 676.
16. Y. Suzuki, Y. Arai, Y. Okamoto and T. Ohmichi, *J. Nucl. Sci. Technol.* **31** (1994) 677.
17. A.J. Bard and L.R. Faulkner, 'Electrochemical Methods: Fundamentals and Applications' (John Wiley & Sons, New York, 1980), chapter 6.
18. V.W. Lorenz, *Z. Naturforsch.* **9A** (1954) 716.
19. L. Yang and R.G. Hudson, *J. Electrochem. Soc.* **106** (1959) 986.
20. I. Barin, 'Thermochemical Data of Pure Substances' (VCH, Weinheim, 3rd edn, 1995) 1234 pp.
21. L.B. Pankratz, 'Thermodynamic Properties of Halides', Bulletin 674 (US Bureau of Mines, Albany, OR (PB84-233329, 1984).
22. G.J. Janz, 'Thermodynamic and Transport Properties for Molten Salts: Correlation Equations for Critically Evaluated Density, Surface Tension, Electrical Conductance, and Viscosity Data' (American Chemical Society and American Institute of Physics, 1988), p. 44.
23. D.M. Kolb, M. Przasnyski and H. Gerischer, *J. Electroanal. Chem.* **54** (1974) 25.
24. H.B. Michaelson, *J. Appl. Phys.* **48** (1977) 4729.
25. S. Trasatti, *J. Electroanal. Chem.* **33** (1971) 351.
26. W. Gordy and W.J.O. Thomas, *J. Chem. Phys.* **24** (1956) 439.